amino acid preparations was between 0.01 and 0.08% (manufacturers specifications). Stepwise chain assembly was carried out in a machine-assisted fashion on a highly modified Applied Biosystems 430A synthesizer (0.2 mmol scale with D- or L-Boc-Phe-OCH_2-Pam-resin). Each cycle of amino acid addition (*9*) involved: Nα-deprotection, neat (100%) trifluoroacetic acid (2 × 30-s flow washes, + 1-min batchwise treatment); *N,N'*-dimethyl formamide (DMF) flow wash (1 × 22 s followed by 1 × 38 s); and coupling (1 × 10 min) with simultaneous in situ neutralization [Boc amino acid (2.25 mmol) preactivated by reaction with benzotriazolyltetramethyluronium-hexafluorophosphate (HBTU) (2.22 mmol) and diisopropylethylamine (DIEA) (6.4 mmol) in DMF for 2 min]. The in situ neutralization method has been shown to result in negligible levels of racemization (*9*) [P. Henklein, M. Beyermann, B. Costisella, R. Sohr, M. Haußner, in *Innovation & Perspectives in Solid Phase Synthesis*, R. Epton, Ed. (SPPC Ltd., Birmingham, U.K., in press)]. The assembled peptides were deprotected and cleaved from the resin in 9:1 HF–*p*-cresol [resorcinol and thiocresol were present when His(Bom) was included in the sequence] after removal of the Boc group and the formyl group from Trp (with ethanolamine) (*8*).

14. After deprotection and cleavage the crude peptide products were precipitated with ether and dissolved with 6 M guanidine hydrochloride in a pH 8.0 $NaHCO_3$ buffer prior to semi-preparative C_{18} reversed-phase high-performance liquid chromatography enrichment and folding by dialysis in 10% glycerol, 25 mM NaH_2PO_4 buffer, pH 7.0 (*10, 11*). After concentration under high vacuum to a solution in glycerol, the enzymes were quantitated by amino acid analysis and stored at 4°C.
15. Samples taken in the assembly of the D-monomer polypeptide chain were cleaved and deprotected, and the sequence was determined by matrix-assisted laser desorption time-of-flight mass spectrometric readout (B. Chait and S. B. H. Kent, unpublished results).
16. The CD spectra from 260 to 195 nm were taken in a pH 5.5 aqueous solution containing 5% glycerol at 25°C with a 1-mm path length quartz cell on an Aviv CD spectrometer.
17. M. V. Toth and G. R. Marshall, *Int. J. Peptide Protein Res.* **36**, 544 (1990). The fluorogenic assays were performed with 15-μl aliquots [corresponding to 1.75 (±10%) μg of protein] of each enzyme enantiomer in 10% glycerol, 100 mM MES buffer, pH 6.5, added to a solution of 50 μM D- or L-fluorogenic substrate in the MES buffer. The substrate sequence was 2-aminobenzoyl-Thr-Ile-Nle-Phe(*p*-NO_2)-Gln-Arg-amide; it was synthesized with either D- or L-amino acid derivatives to provide the appropriate enantiomeric forms.
18. S. B. H. Kent *et al.*, in *Viral Proteinases as Therapeutic Targets*, E. Wimmer and H. G. Kräusslich, Eds. (Cold Spring Harbor Laboratory, Cold Spring Harbor, NY, 1989), pp. 223–230.
19. A. D. Richards, R. Roberts, B. M. Dunn, M. C. Graves, J. Kay, *FEBS Lett.* **247**, 113 (1989).
20. H. G. Kräusslich *et al.*, *Proc. Natl. Acad. Sci. U.S.A.* **86**, 807 (1989).
21. The empty (uncomplexed) HIV PR molecule is highly symmetric and has a C_2 axis; that is, a 180° rotation about an axis running between the flaps and between the active site Asp residues generates an identical structure (*10*). This rotational symmetry does not affect the chiral asymmetry of the enzyme molecule.
22. The L- and D-enzymes in this study have not been exposed to biosynthetic conditions and have thus not been in contact with biochemical factors of any sort. Interestingly, the simple homodimeric enzyme molecule studied here is formed rapidly (both folding and assembly) and accurately even at the relatively low concentrations used in the assay conditions, as well as in more normal dialysis-from-denaturant folding conditions. The results obtained in this study are conclusive evidence that whatever their proposed role, biosynthetic factors are not required for the formation of the correct, functional folded and assembled form of the protein. This result suggests that caution should be exercised in hypotheses concerning biosynthetic oligomeric protein folding [J. E. Rothman, *Cell* **59**, 591 (1989)]. Our observations are consistent with the original proposal [C. B. Anfinsen, *Science* **181**, 223 (1973)] that the amino acid sequence alone determines the folded 3-D form of the protein molecule.
23. Although D-amino acids and small peptides containing D-amino acids may function as haptens in an immune response, it is not expected that a long polypeptide chain made up entirely of D-amino acids could be processed and presented by the immune system.
24. Enzyme enantiomers may have use as chiral catalysts in the production of both enantiomers of a fine chemical.
25. Protein enantiomers can potentially contribute to the acquisition of phase data in x-ray crystallography [A. L. Mackay, *Nature* **342**, 133 (1989)]. Centro-symmetric crystals of a D-, L-protein pair would have greatly simplified phases, and more reliable structures may be obtained in this way.
26. Ribosomal synthesis of polypeptide chains, even in in vitro translation systems, does not incorporate D-amino acids [J. A. Ellman, D. Mendel, P. G. Schultz, *Science* **255**, 197 (1992)].
27. M. Schnölzer and S. B. H. Kent, *Science* **256**, 221 (1992).
28. D. A. Bergman *et al.*, poster presented at the Lorne Conference, Victoria, Australia, 10 February 1992.
29. A. P. Bruins, T. R. Covey, J. D. Henion, *Anal. Chem.* **59**, 2642 (1987).
30. P. J. Kraulis, *J. Appl. Crystallogr.* **24**, 946 (1991).
31. J. S. Richardson and D. C. Richardson, in *Protein Folding*, L. M. Gierasch and J. King, Eds. (American Association for the Advancement of Science, Washington, DC, 1990), pp. 5–17.
32. We thank A. Aguon, G. Verducci, and M. Schnölzer for assistance in the synthesis of the D-substrate; G. Merutka for assistance with CD spectra; and V. Roberts for assistance in preparing Fig. 3. Support of this work by the Markey Foundation is gratefully acknowledged.

5 March 1992; accepted 17 April 1992

Lymphoid Development in Mice Congenitally Lacking T Cell Receptor αβ–Expressing Cells

Karen L. Philpott,* Joanne L. Viney, Graham Kay, Sohaila Rastan, Edith M. Gardiner, Sarah Chae, Adrian C. Hayday, Michael J. Owen

Vertebrate T cells express either an αβ or γδ T cell receptor (TCR). The developmental relatedness of the two cell types is unresolved. $\alpha\beta^+$ T cells respond to specific pathogens by collaborating with immunoglobulin-producing B cells in distinct lymphoid organs such as the spleen and Peyer's patches. The precise influence of $\alpha\beta^+$ T cells on B cell development is poorly understood. To investigate the developmental effects of $\alpha\beta^+$ T cells on B cells and $\gamma\delta^+$ T cells, mice homozygous for a disrupted TCRα gene were generated. The homozygotes showed elimination of $\alpha\beta^+$ T cells and the loss of thymic medullae. Despite this, $\gamma\delta^+$ T cells developed in normal numbers, and there was an increase in splenic B cells.

In all vertebrates examined, T cells express either an αβ TCR or a γδ TCR (*1*). The better understood, αβ TCR, is expressed by most systemic T cells (*1*). It recognizes specific peptides within a polymorphic cleft of major histocompatibility (MHC) antigens (*2*). αβ T cells that populate the peripheral immune system of adult animals are mostly specific for MHC complexed with peptides encoded by foreign agents or pathogens. The effector response to this recognition is variable, depending on largely uncharacterized factors, but the end result is that αβ T cells contribute to the eradication of foreign pathogens by direct cytotoxicity toward infected cells and by the stimulation of B cell production of antigen-specific antibodies (*3*). However, the degree to which B cell development is uniformly dependent on αβ T cells is unclear. Some B cell responses are apparently T cell–independent (*4*), and there may also be a negative influence of T cells on B cell development (*5*). Experiments that examine B cell development in congenitally athymic, nude mice have frequently yielded conflicting results (*6*), presumably because this mutant does not eliminate $\alpha\beta^+$ T cells comprehensively.

In contrast to cells that bear the αβ TCR, the biological function of γδ TCR–bearing cells is unknown. There is strong similarity between the structures of αβ and γδ TCR (*7*), and cell surface expression of both occurs in association with a cluster of proteins termed CD3. γδ T cells that recognize peptides and MHC antigens have

K. L. Philpott, J. L. Viney, M. J. Owen, Imperial Cancer Research Fund, P.O. Box 123, 44 Lincoln's Inn Fields, London WC2A 3PX, United Kingdom.
G. Kay and S. Rastan, Section of Comparative Biology, Medical Research Council Clinical Research Centre, Watford Road, Harrow, Middlesex HA1 3UJ, United Kingdom.
E. M. Gardiner, S. Chae, A. C. Hayday, Department of Biology, Kline Biology Tower, Yale University, 219 Prospect Street, New Haven, CT 06511.

*Present address. EISAI, London Research Laboratories, Darwin Building, Gower Street, London, United Kingdom.

been isolated (8). However, it is difficult to place such cells into a physiologic context until the major biological role of the γδ TCR is determined.

Interestingly, $\alpha\beta^+$ and $\gamma\delta^+$ T cells show developmental dissimilarities. For example, the early murine thymus produces predominantly γδ cells, but this decreases precipitously coincident with the development of αβ thymocytes (9), which suggests their developmental relatedness. Furthermore, particular lymphoid tissues appear to be the domain predominantly of one T cell type or the other (10, 11). For example, $\gamma\delta^+$ cells comprise the major population of the murine skin (12) but are almost entirely absent from Peyer's patches and lymph nodes (13). Again, the basis of this may be developmental regulatory interactions between $\alpha\beta^+$ and $\gamma\delta^+$ T cells, in which case elimination of one type of T cell should lead to compensatory increases in the other.

To clarify the influence of T cells on T and B cell development, several attempts have been made to disrupt the T cell repertoire, such as the depletion of αβ T cells by injection of antibodies specific for αβ T cells (14) and the exclusion of certain types of TCRs by the expression of prerearranged TCR transgenes (15). However, the first rarely gives complete depletion and is difficult to do at early times in lymphoid development. Similarly, the second suffers from variable expressivity of the transgene.

Instead, the most direct way to address these problems is to genetically delete the capacity to make either set of T cells. We disrupted the murine TCRα gene (Fig. 1A). The coding potential of the first C_α exon (CI) was disrupted by insertion of the transposon *Tn5* neomycin resistance gene driven by a eukaryotic promoter. A herpes simplex virus thymidine kinase gene was included to permit negative selection against nonhomologous integration events, although the frequency of homologous integration events (2.5 to 4%) rendered negative selection unnecessary. Embryonal stem (ES) cells (16) were electroporated with the linearized construct, and neomycin-resistant clones with a disrupted TCRα allele were identified by polymerase chain reaction (PCR) analysis (Fig. 1, A and B) and by detection of a novel 2.8-kb Eco RI fragment with Southern (DNA) analysis (Fig. 1, A and C). Two such clones, 129TCRA399 and 129TCRA530, that carried no additional input DNA integrated nonhomologously (17) were injected into BALB/c blastocysts and ten overtly chimeric pups were derived (Table 1). After mating male chimeras generated from the two ES lines to BALB/c females, we scored transmission of the ES cell genome by the birth of agouti/chincilla offspring. Founders transmitted to the germ line with a frequency ranging from 9 to 100% (Table 1). Southern blot analysis of tail DNA (Fig. 1C) showed that about 30% of the agouti offspring inherited a copy of the mutated TCRα allele (Table 1). Such mice were sibling-mated to homozygosity, which was also confirmed by Southern blot analysis (Table 1 and Fig. 1C).

Mice homozygous for the mutant TCRα gene ($TCR\alpha^{-/-}$) were outwardly indistinguishable from heterozygous ($TCR\alpha^{-/+}$) or

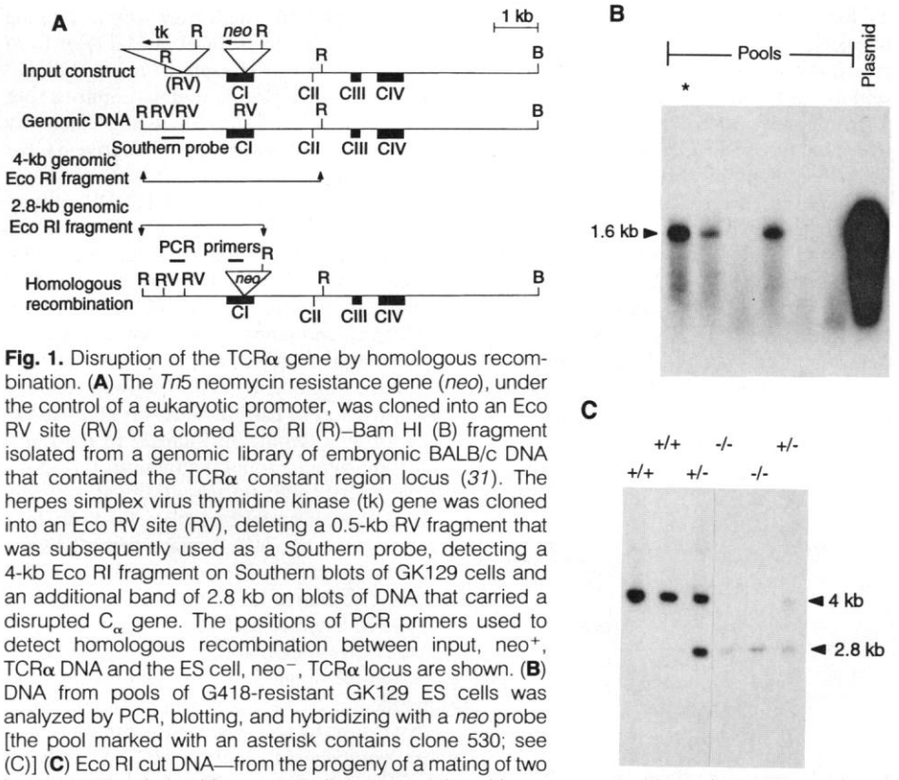

Fig. 1. Disruption of the TCRα gene by homologous recombination. (**A**) The *Tn5* neomycin resistance gene (*neo*), under the control of a eukaryotic promoter, was cloned into an Eco RV site (RV) of a cloned Eco RI (R)–Bam HI (B) fragment isolated from a genomic library of embryonic BALB/c DNA that contained the TCRα constant region locus (31). The herpes simplex virus thymidine kinase (tk) gene was cloned into an Eco RV site (RV), deleting a 0.5-kb RV fragment that was subsequently used as a Southern probe, detecting a 4-kb Eco RI fragment on Southern blots of GK129 cells and an additional band of 2.8 kb on blots of DNA that carried a disrupted C_α gene. The positions of PCR primers used to detect homologous recombination between input, neo^+, TCRα DNA and the ES cell, neo^-, TCRα locus are shown. (**B**) DNA from pools of G418-resistant GK129 ES cells was analyzed by PCR, blotting, and hybridizing with a *neo* probe [the pool marked with an asterisk contains clone 530; see (C)] (**C**) Eco RI cut DNA—from the progeny of a mating of two heterozygotes derived from a germ line–transmitting chimera generated from clone 530—analyzed by Southern blot with the 0.5-kb Eco RV probe shown in (A). Representative +/+, +/−, and −/− littermates are shown.

Table 1. Generation of overt chimeras with ES clones 530 and 399.

	Cell line			
	Clone 530			Clone 399
Blastocysts injected (*n*)*	67			27
Progeny born (% blastocysts transferred)	32 (48%)			2 (7.5%)
Chimeras (% of progeny born)	8 (25%)			2 (100%)
Sex (male, female)	5, 3			1, 1
Individual transmitting chimeras (approximate % coat-color chimerism)†	530/1 (90%)	530/2 (20%)	530/5 (20%)	399/1 (40%)
ES cell–derived progeny/total progeny (% transmission)‡	26/27 (96%)	2/21 (9.5%)	7/12 (58%)	11/11 (100%)
$TCR\alpha^{-/+}$ genotype§	7‖	0	1	5

*Ten to 15 ES cells were injected into BALB/c blastocysts and transferred to the uteri of pseudopregnant recipients. †Assessed by the contribution of pale yellow color from GK129 cells (129/Ola/Hsd strain carrying pigment genes $A^wBc^{ch}p$). ‡Assessed by the contribution of pigment genes carried by 129/Ola/Hsd strain in the F1 progeny of chimeras mated to BALB/c females. §Assessed by Southern analysis (Fig. 1C). ‖$TCR\alpha^{-/+}$ mice were subsequently sibling-mated to yield homozygous $TCR\alpha^{-/-}$ mice, from which breeding pairs have been established.

Table 2. Cell yields.

Organ	Cell type		
	+/+	−/+	−/−
Thymus*	1.3×10^8	1.3×10^8	8.8×10^7
Spleen*	1.1×10^8	1.1×10^8	9.6×10^7
Peyer's patches†	2.2×10^6	2.1×10^6	8.8×10^5

*Average number per animal. †Average number per Peyer's patch.

wild-type ($TCR\alpha^{+/+}$) littermates. Thymi and spleens from $TCR\alpha^{-/-}$ mice were of approximately normal size and contained normal numbers of cells (Table 2). In contrast, Peyer's patches in $TCR\alpha^{-/-}$ mice were smaller, shriveled in appearance, and barely discernible in comparison to those in $TCR\alpha^{-/+}$ or $TCR\alpha^{+/+}$ siblings (Table 2). We examined the phenotypes of cells in the thymus, spleen, and Peyer's patches with fluorescence-activated cell sorter (FACS) analysis, using monoclonal antibodies (MAbs) to a variety of lymphocyte cell surface proteins.

Table 3. Percentage of hematopoietic cells in spleens and Peyer's patches that stained for surface antigens. Blank spaces indicate that double stainings were not performed on Peyer's patch samples.

Surface antigens	Spleen		Peyer's patches	
	+/+	−/−	+/+	−/−
Ig	56.3*	80.9	29.6	80.0
CD3	32.5	4.2	61.4	2.9
αβ TCR	30.4	< 1	60.5	< 1
γδ TCR	2.0	3.6	< 1	1.2
CD4	19.8	1.5	49.6	< 1
CD8	8.8	< 1	5.4	< 1
CD4, γδ TCR	< 1	< 1		
$CD4^-$, γδ TCR	2.6	3.7		
CD8, γδ TCR	< 1	< 1		
Thy-1	35.2	2.4		

*Values are means of five samples.

Complete elimination of $\alpha\beta^+$ T cells from $TCR\alpha^{-/-}$ mice was evident from the failure of any cells to react with an αβ TCR–specific MAb (H57.597) that recognized the C_β region (*18*) (Fig. 2, A and B, and Table 3). The residual $CD3^+$ cells in these mice were $\gamma\delta^+$ T cells that occurred in approximately normal numbers in comparison to those from $TCR\alpha^{-/+}$ or $TCR\alpha^{+/+}$ siblings (Fig. 2B and Table 3). Furthermore, the splenic $\gamma\delta^+$ cells in $TCR\alpha^{-/-}$ mice had a normal cell surface phenotype, in that they were double negative (DN) for CD4 and the CD8 glycoprotein co-receptors (Table 3). No alternative forms of TCR, such as the βδ heterodimer in a human cell line (*19*), were detectable by FACS analysis among $TCR\alpha^{-/-}$ cells. Furthermore, an extensive immunohistological analysis with enzyme-linked and fluorescence-labeled antibodies failed to detect unequivocally $CD3^+$ cells that expressed surface TCR β chain, either alone or together with TCRδ. Hence, the engineered mutation in TCR C_α congenitally eradicated murine αβ cells without creating any other obvious perturbations of the mature T cell repertoire.

The thymi of $TCR\alpha^{-/-}$ mice were approximately normal in size in comparison to those of $TCR\alpha^{-/+}$ and $TCR\alpha^{+/+}$ siblings. FACS analysis of $TCR\alpha^{-/-}$ thymocytes showed that this was because there was no reduction in the number of cells double positive (DP) for CD4 and CD8, ordinarily the most abundant cell type in the thymus (Fig. 2A). DP cells, which arise after the $CD4^{low}$, DN, and $CD8^{low}$ stages, occur in a mid to late stage of T cell development during which the cell surface expression of αβ TCR matures from negative through low to high (*20*). Cells in the last of these categories are then subject to selection, coincident with which they switch to being single positive (SP) for either CD4 or CD8 alone (*20, 21*). The predominance of DP cells in the $TCR\alpha^{-/-}$ thymus confirms that this stage of T cell development is efficiently reached in the absence of productive TCRα expression. However, there is no evidence for progression of these TCR^-,DP cells to become TCR^-,SP cells (Fig. 2A).

Spleens in $TCR\alpha^{-/-}$ mice were also approximately normal in size compared to those in $TCR\alpha^{-/+}$ and $TCR\alpha^{+/+}$ mice. This was surprising, given that ordinarily a substantial fraction of splenocytes are $\alpha\beta^+$ T cells. Analysis by FACS showed that the elimination of $\alpha\beta^+$ T cells was compensated for by a significant increase in the number of splenic immunoglobulin (Ig)–positive cells (Table 3). Essentially all of these B cells were surface-positive for both IgM and IgD (Fig. 2C), a state regarded as a precursor of antigen-activated, germinal center B blasts (*22*). Hence, in the complete absence of $\alpha\beta^+$ T cells and the cytokines that they make, B cells of this developmental stage both developed and expanded. The capacity of IgM^+IgD^+ B cell expansion to compensate for the reduction in numbers of splenic $\alpha\beta^+$ T cells in $TCR\alpha^{-/-}$ mice stands in stark contrast to the maintenance of normal numbers of peripheral $\gamma\delta^+$ T cells (Fig. 2B).

A small number of $CD4^+$ cells could frequently be found in $TCR\alpha^{-/-}$ spleens (Table 3). However, both by FACS and by immunohistochemistry, we determined that these cells were $CD3^-$, $TCR\beta^-$, $TCR\gamma\delta^-$, and Ig^-. Therefore, they must be included in the splenic "non-T, non-B" population that is slightly enlarged in $TCR\alpha^{-/-}$ mice, accounting for up to 15% of cells.

Elimination of $\alpha\beta^+$ T cells in $TCR\alpha^{-/-}$ mice resulted in Peyer's patches that were less than half the size of those in $TCR\alpha^{-/+}$ and $TCR\alpha^{+/+}$ siblings (Table 2). Analysis by FACS showed that Peyer's patch B cells that had surface Ig were present in approximately normal numbers (Table 3). The degree to which T cell help is required for Peyer's patch B cell expansion and maturation is contentious (*23*). For example, in congenitally athymic, nude mice, B cells

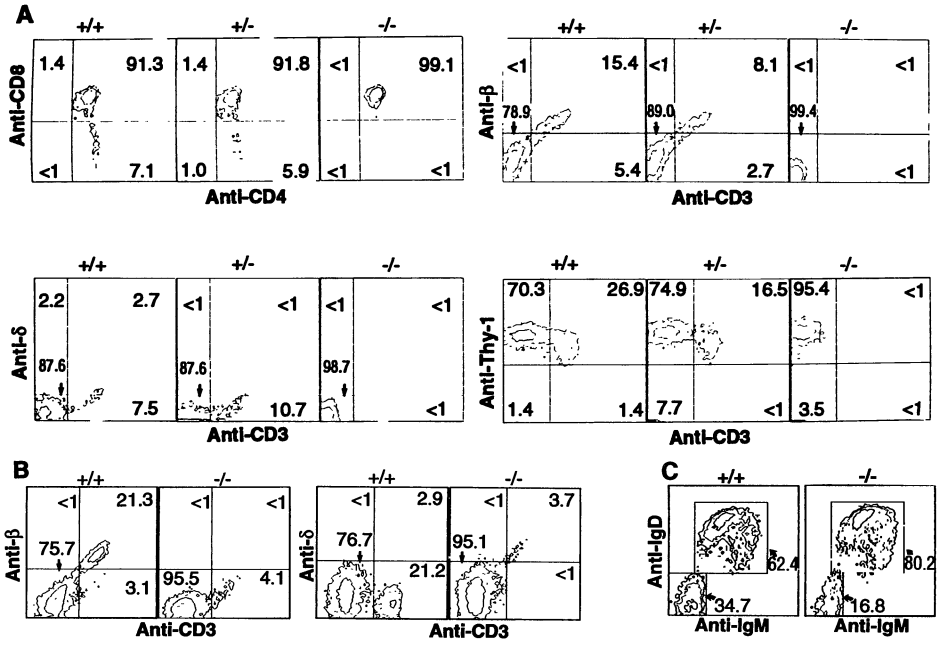

Fig. 2. Phenotypes of $TCR\alpha^{-/-}$ lymphocytes compared with those in normal littermates. (**A**) Thymocytes isolated from $TCR\alpha^{+/+}$, $TCR\alpha^{-/+}$, and $TCR\alpha^{-/-}$ mice were stained with phycoerythrin (PE)-conjugated GK1.5 (rat MAb to mouse CD4) (*32*); fluoresceinated 53-6.72 (rat MAb to mouse CD8) (*33*); biotinylated H57.597 (hamster MAb to mouse TCRβ) (*18*) or GL3 (hamster MAb to mouse TCRδ) (*34*) and then with PE-streptavidin; or fluoresceinated rat MAb to mouse CD3 (YCD3-1) (*35*) or MAb YTS154 (rat anti-mouse Thy-1) (*36*) and then with PE-conjugated antibodies to rat Ig. Stained and unstained cells were distinguished with a FACScan cytofluorograph. (**B**) Splenocytes stained with MAb 2C11 (anti-CD3) and with either MAb H57 (pan anti-TCRαβ) or MAb GL3 (pan anti-TCRγδ). (**C**) Splenocytes from $TCR\alpha^{+/+}$ and $TCR\alpha^{-/-}$ mice were stained for surface IgM and for surface IgD and analyzed with a FACScan cytofluorograph.

expand, and the Peyer's patches are close to normal size. However, Peyer's patches in nude mice additionally contain αβ T cells (*5, 24*), which may or may not drive Peyer's patch B cell expansion. By contrast, our findings in the TCRα$^{-/-}$ mice showed that in the complete absence of αβ T cell help, normal numbers of Peyer's patch B cells developed but that, unlike in the spleen, they did not expand to compensate for the deficiency in αβ T cell numbers.

The effects of congenital deficiency in αβ$^+$ T cells on the internal anatomy of the thymus, spleen, and Peyer's patches were examined histologically and immunohistochemically (Fig. 3). The most dramatic changes were evident in the thymi of TCRα$^{-/-}$ mice that, compared to wild-type thymi, had grossly expanded cortices packed with DP cells (detected with a MAb to CD8) and no detectable medullae that would ordinarily be scattered with mature, CD8$^+$ cells. In contrast, the TCRα$^{-/-}$ spleens and Peyer's patches retained grossly normal internal anatomy. In TCRα$^{-/-}$ and TCRα$^{+/+}$ spleens, darkly staining lymphoid areas of white pulp occurred among lightly staining blood cell areas of red pulp. However, MAbs to CD3 revealed that the densely populated, periarteriolar T cell areas of TCRα$^{+/+}$ mice were only sparsely populated in TCRα$^{-/-}$ mice with residual CD3$^+$,γδ$^+$ cells. Similarly, the regions between the B cell follicles in the Peyer's patches of TCRα$^{+/+}$ mice that stained densely for CD3 were anatomically discernible but poorly stained with anti-CD3 in TCRα$^{-/-}$ mice.

The construction by homologous recombination of mice that lack the TCRα gene product has allowed several conclusions about thymic development and peripheral lymphoid anatomy to be drawn. Unlike nude mice, in which an epithelial defect leads to serious alterations in αβ and γδ repertoires (*25*), the lymphoid phenotype in TCRα$^{-/-}$ mice can be attributed to an inability to produce αβ T cells. First, in the absence of functional C_α, essentially no mature CD3$^+$ cells form other than CD3$^+$,γδ$^+$ cells. Most TCRα$^{-/-}$ thymocytes arrest at a CD4$^+$CD8$^+$ stage. Arrest of cells at a DP stage was seen in mice transgenic for TCRs that could not be positively selected (*21*). However, those TCR$^+$ cells may have been subject to programmed cell death, to which there is no evidence that DP,TCR$^-$ cells are susceptible. Instead, our results suggest that in the absence of αβ TCR expression, there is no developmental clock measured in time or cell divisions (*26*) that directs DP cells to SP cells.

The confinement of arrested TCR$^-$,DP cells to the thymic cortices of TCRα$^{-/-}$ mice is similar to the cortical localization of TCR$^+$,DP cells that cannot be positively selected (*21*). Beyond this, however, the TCRα$^{-/-}$ mice demonstrate that in the congenital absence of mature αβ$^+$ T cells, there are no discernible thymic medullae. It may be that the thymic medulla is directly induced by αβ$^+$ T cells.

The presence in TCRα$^{-/-}$ mice of approximately normal numbers of γδ$^+$ T cells suggests that such cells can mature from the thymus in the absence of significant medulla. This may be related to the fact that subsets of γδ$^+$ T cells may mature from the murine fetal thymus at a time (embryonic day 16) when the medulla is barely discernible (*9*). The TCRα$^{-/-}$ mice therefore add genetic foundation to the concept that αβ T cells and γδ T cells have distinct developmental and physiological phenotypes (*10, 27*). This is reinforced by the absence of any γδ expansion in the spleen and Peyer's patches that might compensate for the elimination of αβ$^+$ T cells. The retention of essentially normal numbers of γδ$^+$ T

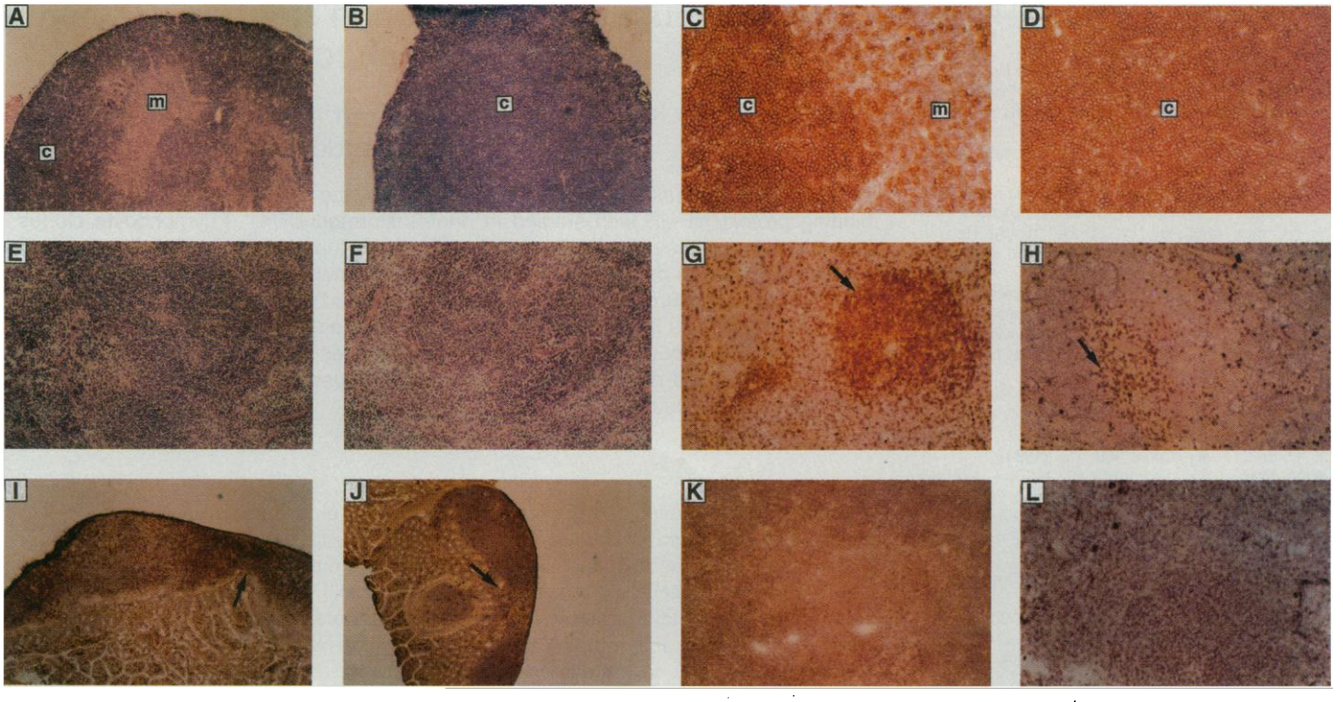

Fig. 3. Immunohistochemical analysis of frozen sections of thymus, spleen, and Peyer's patches. (**A** and **B**) Thymus (×200) stained with hematoxylin and eosin (h and e). (**C** and **D**) Thymus (×600) stained with immunoperoxidase-linked MAbs to CD8. (**E** and **F**) Spleen (×200) stained with h and e. (**G** and **H**) Spleen (×400) stained with immunoperoxidase-linked MAbs to CD3. (**I** and **J**) Peyer's patches (×200) stained with immunoperoxidase-linked anti-CD3 MAbs. (**K**) Thymus (×600) stained with immunoperoxidase-linked MAb to TCRβ (H57.597). (**L**) Spleen (×400) stained with immunoperoxidase-conjugated MAb to TCRβ (H57.597). (A), (C), (E), (G), and (I) are from TCRα$^{+/+}$ mice; (B), (D), (F), (H), (J), (K), and (L) are from TCRα$^{-/-}$ mice; c, cortex; m, medulla. Arrow in (G) shows densely populated, periarteriolar T cell areas of TCRα$^{+/+}$ mice; arrow in (H) shows same area sparsely populated in TCRα$^{-/-}$ mice. Arrow in (I) shows regions between B cell follicles in the Peyer's patches of TCRα$^{+/+}$ mice that stained densely for CD3; arrow in (J) shows poor staining of same area with anti-CD3 in TCRα$^{-/-}$ mice.

cells renders the TCR$\alpha^{-/-}$ mouse an invaluable animal model for the study of γδ cell function. In particular, these mice can potentially resolve whether γδ cells provide, as hypothesized, a response to a broad range of epithelial insults (*10*) and whether they respond, as suggested, to specific pathogens such as mycobacteria (*28*), or both.

The development of B cells in the absence of $\alpha\beta^+$ T cells is consistent with the independent development of the humoral and cell-mediated immune systems (*29*). However, the de facto influence of T cells on B cell development is poorly understood. Our data indicate that TCR$\alpha^{-/-}$ mice will be useful in resolving this; unlike in nude mice, in which spleens and Peyer's patches are approximately normal in size, the complete elimination of $\alpha\beta^+$ T cells has dichotomous effects on B cell development in the spleen and Peyer's patches. Whether this dichotomy is a result of anatomy or whether it is a result of direct effects of $\alpha\beta^+$ T cells on B cell development (for example, negative regulation) that are different in the two organs can now be directly tested.

REFERENCES AND NOTES

1. H. Clevers, B. Alarcon, T. Wileman, C. Terhorst, *Annu. Rev. Immunol.* **6**, 629 (1988); R. D. Klausner, J. Lippincott-Schwartz, J. S. Bonifacino, *Annu. Rev. Cell Biol.* **6**, 403 (1990); M. B. Brenner *et al.*, *Nature* **322**, 145 (1986).
2. D. R. Madden, J. C. Gorga, J. L. Strominger, D. C. Wiley, *Nature* **353**, 321 (1991); A. Y. Rudensky, P. Preston-Hurlburt, S-C. Hong, A. Barlow, C. A. Janeway, Jr., *ibid.*, p. 622.
3. H. Kawanishi, L. Saltzman, W. Strober, *J. Exp. Med.* **157**, 433 (1983).
4. J. J. Cebra, J. A. Fuhrman, P. J. Gaerhart, J. L. Horwitz, R. D. Shahin, in *Recent Advances in Mucosal Immunity*, W. Strober, L. A. Hanson, K. W. Sell, Eds. (Raven, New York, 1982), pp. 155–171.
5. R. M. Ikeda and M. E. Gershwin, in *Animal Models of Comparative and Developmental Aspects of Immunity and Diseases*, M. E. Gershwin and E. L. Cooper, Eds. (Pergamon, Elmsford, NY, 1978), pp. 201–210.
6. J. J. Cebra *et al.*, *Ann. N.Y. Acad. Sci.* **409**, 25 (1983); P. K. Mongini, W. E. Paul, E. S. Metcalf, *J. Exp. Med.* **157**, 69 (1983).
7. H. Saito *et al.*, *Nature* **309**, 757 (1984).
8. W. Born *et al.*, *Science* **249**, 67 (1990); L. A. Matis, R. Cron, J. A. Bluestone, *Nature* **330**, 262 (1987); D. Vidović *et al.*, *ibid.* **340**, 646 (1989).
9. W. L. Havran and J. P. Allison, *Nature* **335**, 443 (1988).
10. C. A. Janeway, Jr., B. Jones, A. Hayday, *Immunol. Today* **9**, 73 (1988).
11. S. Itohara *et al.*, *Nature* **343**, 754 (1990).
12. W. A. Kuziel *et al.*, *ibid.* **328**, 263 (1987); G. Stingl *et al.*, *Proc. Natl. Acad. Sci. U.S.A.* **84**, 4586 (1987).
13. C. R. MacKay and W. R. Hein, *Res. Immunol.* **141**, 611 (1990).
14. A. Carbone *et al.*, *Immunol. Rev.* **120**, 35 (1990); P. F. Mixter, B. C. Sydora, R. M. Hershberg, M. Kronenberg, *J. Immunol.* **147**, 4109 (1991).
15. M. Bonneville *et al.*, *Nature* **342**, 931 (1989).
16. The male ES cell line, GK129 derived from a 129/0la/Hsd strain mouse (*30*) was maintained on mitomycin-treated STO feeder cells supplemented with leukemia inhibitory factor (10^3 U/ml) (ESGRO, Amrad, Australia). Cells (2×10^7) at passage 8 were trypsinized, washed with phosphate-buffered saline, and resuspended at 2.7×10^7 cells per milliliter. The DNA construct shown in Fig. 1 was linearized at the Not I site of the polylinker, and cells were transformed with 20 μg of linearized plasmid with a Bio-Rad electroporater at 0.2 V and 500 μF. After electroporation, ES cells were plated onto a feeder layer of G418-resistant STO cells, and resistant ES cell clones were selected by the addition of G418 (Gibco, Grand Island, NY) (200 μg/ml) beginning 2 days after electroporation. Cells were re-fed with G418-containing media every 2 days. Three hundred eighty G418-resistant colonies (1 in 5×10^4) were visible 10 days after addition of selective medium. Colonies were picked into 24-well plates, and pools of 10 were generated from half of each colony for DNA analysis. Pools that contained homologous integration events were identified by PCR analysis with the primers shown in Fig. 1. ES clones from positive pools were analyzed individually. Positive clones were grown for two further passages before being injected into blastocysts.
17. K. L. Philpott, J. L. Viney, G. Kay, M. J. Owen, unpublished data.
18. R. Kubo, W. Born, J. Kappler, P. Marrack, M. Pigeon, *J. Immunol.* **142**, 2736 (1989).
19. F. Hochstenbach and M. B. Brenner, *Nature* **340**, 562 (1989).
20. C. J. Guidos, J. S. Danska, C. G. Fathman, I. L. Weissman, *J. Exp. Med.* **172**, 835 (1990).
21. H. S. Teh *et al.*, *Nature* **335**, 229 (1988); L. J. Berg *et al.*, *Cell* **58**, 1035 (1989).
22. E. C. Butcher and I. L. Weissman, in *Fundamental Immunology*, W. E. Paul, Ed. (Raven, New York, ed. 2, 1989) pp. 117–138.
23. W. Strober and D. Jacobs, *Adv. Host Def. Mech.* **4**, 1 (1985).
24. A. C. Hayday and S. Roberts, unpublished data.
25. W. L. Havran and J. P. Allison, *Nature* **344**, 68 (1990); S. Carding *et al.*, *Genes Dev.* **4**, 1304 (1990).
26. M. C. Raff, E. R. Abney, J. Fok-Seang, *Cell* **42**, 61 (1985).
27. A. C. Hayday, in *Encyclopedia of Immunology*, I. Roitt and P. Delves Eds. (Saunders, Philadelphia, in press).
28. E. M. Janis, S. E. Kaufmann, R. H. Schwartz, D. M. Pardoll, *Science* **244**, 713 (1989).
29. B. Glick, T. S. Chang, R. G. Jaap, *Poult Sci.* **35**, 224 (1956); J. F. A. P. Miller, *Lancet* ii, 748 (1961).
30. G. Kay, unpublished data.
31. A. C. Hayday *et al.*, *Nature* **316**, 828 (1985).
32. D. P. Dialynas *et al.*, *Immunol. Rev.* **74**, 29 (1983).
33. J. A. Ledbetter, R. V. Rouse, H. S. Micklem, L. A. Herzenberg, *J. Exp. Med.* **152**, 280 (1980).
34. T. Goodman and L. Lefrancois, *ibid.* **170**, 1569 (1990).
35. P. Portoles *et al.*, *J. Immunol.* **142**, 4169 (1989).
36. S. P. Cobbold, S. Thierfelder, H. Waldmann, *Mol. Biol. Med.* **1**, 285 (1983).

37. We thank G. Klaus and D. Gray for reagents; R. Flavell, E. Elliot, G. Warren, and P. Askenase for encouragement; and R. Beddington for help and advice during the early stages of this work. Supported by the Imperial Cancer Research Fund, by Medical Research Council grants to S.R., and by NIH grant GM37759 to A.C.H. All experiments involving animals were conducted in accredited animal quarters after review and approval by the appropriate Animal Care Committees. This report is dedicated to the memory of Alan Williams who made immunoglobulin domains so much fun for so many of us.

20 March 1992; accepted 6 May 1992

NF-κB Subunit Regulation in Nontransformed CD4$^+$ T Lymphocytes

Sang-Mo Kang,* Annie-Chen Tran, Mariagrazia Grilli,† Michael J. Lenardo‡

Regulation of interleukin-2 (IL-2) gene expression by the p50 and p65 subunits of the DNA binding protein NF-κB was studied in nontransformed CD4$^+$ T lymphocyte clones. A homodimeric complex of the NF-κB p50 subunit was found in resting T cells. The amount of p50-p50 complex decreased after full antigenic stimulation, whereas the amount of the NF-κB p50-p65 heterodimer was increased. Increased expression of the IL-2 gene and activity of the IL-2 κB DNA binding site correlated with a decrease in the p50-p50 complex. Overexpression of p50 repressed IL-2 promoter expression. The switch from p50-p50 to p50-p65 complexes depended on a protein that caused sequestration of the p50-p50 complex in the nucleus.

Tumor cell lines have proven vital to the study of gene regulation because they are easily grown and manipulated. However, nontransformed T cells exhibit biological characteristics that are not manifested by T cell tumor cell lines, including proliferative responses to antigen, costimulatory requirements, clonal anergy, and propriocidal regulation (*1–5*). Therefore we used major histocompatibility complex (MHC)–restricted T lymphocyte clones that faithfully recapitulate the in vivo cellular response to peptide antigen (*1–5*). These clones are neither transformed nor immortalized and survive in culture by stimulation with antigen and antigen-presenting cells (APCs). T cell clones have not been widely used for gene regulation studies because they appeared to be refractory to DNA transfection and because natural antigen stimulation requires a two-cell interaction with antigen-presenting cells. We devised methods

Laboratory of Immunology, National Institute for Allergy and Infectious Diseases, National Institutes of Health, Bethesda, MD 20892.

*Present address: Department of Surgery, University of California, San Francisco, CA 94143.
†Present address: Institute of Pharmacology, Department of Biomedical Sciences and Biotechnology, University of Brescia Medical School, Brescia, Italy.
‡To whom correspondence should be addressed.